Oral Oncology 96 (2019) 131–139

Contents lists available at ScienceDirect

Oral Oncology

journal homepage: www.elsevier.com/locate/oraloncology

pDC depletion induced by CD317 blockade drives the antitumor immune response in head and neck squamous cell carcinoma

Lei-Lei Yang[a], Liang Mao[a], Hao Wu[a], Lei Chen[a], Wei-Wei Deng[a], Yao Xiao[a], Hao Li[a], Lu Zhang[b,*], Zhi-Jun Sun[a,b,*]

[a] The State Key Laboratory Breeding Base of Basic Science of Stomatology (Hubei- MOST) & Key Laboratory of Oral Biomedicine Ministry of Education, School & Hospital of Stomatology, Wuhan University, Wuhan, China
[b] Department of Oral Maxillofacial-Head Neck Oncology, School and Hospital of Stomatology, Wuhan University, Wuhan, China

ARTICLE INFO

Keywords:
Head and neck cancer
Plasmacytoid dendritic cells
Immunosuppressive cells
Immune checkpoints
Transgenic mouse model
Tissue microarray

ABSTRACT

Objectives: Dysregulation of immune cells in the tumor microenvironment is a hallmark of head and neck squamous cell carcinoma (HNSCC). Increased infiltration of pDCs has been reported in the microenvironment of HNSCC. However, the precise immunological role of pDC and the therapeutic effects of pDC depletion in HNSCC need to be further investigated.

Materials and methods: CD317 antibodies were applied for depleting pDCs in an immunocompetent transgenic HNSCC mouse model. Tumor volume was monitored. Flow cytometric analysis was conducted for studying the immune profile changes after pDC depletion. In addition, immunohistochemical staining was carried out in a human HNSCC tissue microarray for detecting the infiltration of pDCs. We also analyzed the survival implication of pDCs and its correlation with other immune related markers in human HNSCC.

Results: pDC depletion in the transgenic HNSCC mouse model significantly delayed tumor growth. After pDCs were depleted, T cells were markedly revitalized, and the proportions of regulatory T cells (Tregs) and monocytic myeloid-derived suppressor cells (MDSCs) were decreased. In human HNSCC microenvironment, pDC infiltration was upregulated and its high infiltration conferred a poor prognosis. Moreover, pDC infiltration was closely correlated with the expression of Foxp-3, PD-1, TIM-3, and LAG-3.

Conclusion: Our findings demonstrated that pDCs play a negative immunomodulatory role in HNSCC and may present as a target for effective immunotherapy.

Introduction

Head and neck squamous cell carcinoma (HNSCC) is a prevalent malignancy, with an incidence of almost 550,000 new cases a year [1]. The relatively unchanged high mortality rates of about 40–50% [2], as well as the functional defects and disfiguring consequences caused by surgical therapy, force us to develop more effective approaches and modalities.

Recently, the dysregulated immune microenvironment's role in tumor evolution and progression has attracted great attention [3]. Immunomodulatory cell types, such as Tregs, myeloid-derived suppressor cells (MDSCs), and M2 macrophages can result in immune evasion through multiple pathways in the tumor milieu of HNSCC [4]. Tregs are highly accumulated in HNSCC patients and potently inhibit T cell proliferation [5]. MDSCs represent a heterogeneous cell population and have been categorized as polymorphonuclear MDSCs ($CD11b^+Ly6G^{high}Ly6C^{low}$) and monocytic MDSCs ($CD11b^+Ly6G^-Ly6C^{high}$) [6]. MDSCs remarkably suppress the anti-tumor T cell response through multiple pathways [7]. In addition, immune checkpoints can also be exploited by tumor in preventing immune destruction [8,9]. Studies in our laboratory and other laboratories have established that immune checkpoints, such as PD-1 (programmed death-1), LAG-3 (lymphocyte activation gene 3) and TIM-3 (T-cell immunoglobulin and mucin-domain containing-3), lead to immune suppression in HNSCC [10–13]. The upregulated expression of these immune checkpoints is associated with the induction of the T cell exhaustion state [14].

Plasmacytoid dendritic cells (pDCs) are a distinct subtype of DCs. The C-type lectin BDCA2 (CD303) is specifically expressed by pDCs in humans [15]. However, in mice, pDCs are characterized as $B220^+CD11c^{low}CD317^+$ cells [16]. pDCs contribute to the antiviral immune response by producing large amounts of type I interferons (IFNα/β) [17]. However, emerging evidence suggests that pDCs have a

* Corresponding authors at: School and Hospital of Stomatology, Wuhan University, 237 Luoyu Road, Wuhan 430079, China.
E-mail addresses: luzhang2012@whu.edu.cn (L. Zhang), sunzj@whu.edu.cn (Z.-J. Sun).

https://doi.org/10.1016/j.oraloncology.2019.07.019
Received 12 March 2019; Received in revised form 16 July 2019; Accepted 23 July 2019
Available online 26 July 2019
1368-8375/

divergent role in tumor microenvironments [16,18]. Tumor-associated pDCs often display an immature state [19], and their accumulation indicates poor prognosis in melanoma and ovarian cancer [20,21]. In the HNSCC microenvironment, the capacity of pDCs to secret type I IFNs is suppressed, and promote regulatory $CD8^+$ T cells [22]. However, the specific immune-related signature of pDCs and the possibility of pDC depletion as a treatment for head and neck cancer needs to be further investigated.

The purpose of this study was to determine whether the immunosuppressive status in a tumor-bearing immunocompetent HNSCC model would be ameliorated after pDC depletion. Furthermore, the associations of pDCs with the immune status and progression of human HNSCC were explored.

Materials and methods

Detailed materials and methods please see supplementary file.

Immunocompetent HNSCC murine model

Animal experiments were conducted according to the guidelines of the National Institutes of Health Guidelines. This study was also approved by Institutional Animal Care and Use Committee of Wuhan University (approval number: 2016LUNSHENZI62). Mice with *Tgfbr1/Pten* double gene conditional knockout (*Tgfbr1*$^{flox/flox}$, *Pten*$^{flox/flox}$, and *K14-CreER*$^{tam+/-}$) were used for this study. After tamoxifen applied, this mouse model can develop head neck epithelial and oral mucosa tissue-specific squamous cell carcinoma as previously described [23]. Supplementary file will provide detailed information.

Tumor induction and pDC depletion

Tamoxifen was applied to the oral mucosa of *Tgfbr1/Pten* conditional knockout (2cKO) mice to induce squamous cell carcinoma as previously described [24]. The in vivo CD317 monoclonal antibodies (Clone: 927, Catalog # BE0311) and isotype control (in vivo mAb rat Rat IgG2b, isotype control) antibodies for the in vivo depletion of pDC were purchased from Bio X Cell (West Lebanon, NH, USA) [25–27]. The antibodies were diluted and assigned to a control group (in vivo mAb rat IgG2b isotype control, 15 mg/kg, Bio X Cell, i.p., q.o.d., n = 6 mice) and a pDC depletion group (in vivo CD317 monoclonal antibody, 15 mg/kg, i.p., q.o.d., n = 6 mice). Supplementary file will provide detailed information.

Flow cytometry for mouse tissue

Mouse tumor tissue, spleens, draining lymph nodes and blood were harvested and prepared for flow cytometric analysis using CytoFLEX flow Cytometer (Beckman Coulter). The following fluorochrome-conjugated antibodies were used: isotype-matched IgG controls, CD4 FITC, CD8 PerCPCy5.5, CD11c APC, CD45 PE-Cy7, B220 FITC, CD317 PE, TIM-3 APC, PD-1 BV421, LAG-3 PE, FOXP-3 PE, CD11b FITC, Ly6C PE-Cy7, Ly6G PE (all from eBioscience, San Diego, CA). CytExpert software (Beckman Coulter) was used to analyze cell surface markers and intracellular protein expression. Supplementary file will provide detailed information.

Collection of human tumor infiltrating lymphocytes and flow cytometry analysis

All procedures involving human performed in this project were permitted by the Institutional Review Board of the School and Hospital of Stomatology, Wuhan University (approval number: 2016LUNSHENZI62). Written informed consent forms were signed by all participants before they underwent surgery. Fresh HNSCC samples were obtain from the 5 patients who receive surgery in school and hospital of stomatology, Wuhan University. Tumor samples were dissociated, enzymatically digested, and collected by density gradient centrifugation method. For flow cytometry analysis, the following fluorochrome-conjugated antibodies were used: isotype-matched IgG controls, CD45 APC-eFluor 780 (eBioscience, San Diego, CA), CD123 BV421 (BioLenged, San Diego, CA), CD303 APC (BioLenged), CD80 FITC (BioLenged).

Patients selection and tissue microarray construction

Cylindrical cores (1.5 mm) were punched from representative tumor or epithelial areas of each patient's tissue samples and were assembled into HNSCC tissue microarrays. 210 primary HNSCC samples, 69 dysplasia samples, and 42 normal mucosa samples were included in this human HNSCC microarray. The tissue microarray also contained 15 HNSCC samples with a history of presurgical radiotherapy and 20 HNSCC samples with a history of inductive TPF chemotherapy (Taxol, platinum and 5-fluorouracil). A part of HNSCC patients in this study have been described by Dr. Wu L in the Supporting Information [28]. The detailed information of the rest 94 cases has been provided in Table S1. Supplementary file will provide detailed information.

Immunohistochemical and immunofluorescence staining

Immunohistochemical staining was performed as previously described [24]. Specific primary antibodies including PD-1, Foxp3, CD4, CD8, TIM-3, LAG-3, Ki-67, Granzyme B, and isotype controls (all from Cell Signaling Technology, Danvers, MA, USA). CD303 form R&D Systems (Minneapolis, MN, USA) and Perforin from Abcam (Cambridge, UK) were also used. The steps for the immunofluorescence were the same as those for immunohistochemistry staining before adding fluorochrome conjugated secondary antibodies. Ki-67 from Cell Signaling Technology and CD303 antibodies were used. Sections were incubated with corresponding fluorescent antibodies (DyLight 594 anti-goat and DyLight 488 anti-rabbit; Thermo Fisher Scientifc, Waltham, MA, USA) for 1 h in the dark at 37 °C and then mounted with DAPI. The slides were observed by a fluorescence microscope (CLSM-310, ZEISS fluorescence microscope, Germany). Supplementary file will provide detailed information.

Image analyses and hierarchical clustering

All the slides were digitized by the Aperio ScanScope CS2 scanner. Aperio quantification software was used to quantify the staining of immunohistochemical slides as previously described [24,29]. For hierarchical clustering, Cluster 3.0 and Java TreeView 1.0.5 were used for calculation and presentation as previously described [12]. Supplementary file will provide detailed information.

Statistical methods

GraphPad Prism 7.0 (GraphPad Software, Inc., La Jolla, CA) for Windows was used to process data analysis. The Kaplan–Meier curves were plotted and analyzed by log-rank test for overall survival of CD303 expression level. The correlation analysis among CD303 with PD-1, TIM-3, LAG-3 and Foxp3 was evaluated through two-tailed Pearson correlation. Supplementary file will provide detailed information.

Results

CD317 blockade effectively depleted pDCs and retarded tumor growth

Dysregulation of the PTEN/PI3K/Akt and TGF-β signaling pathways is common in human HNSCC [30]. In the head and neck epithelia and oral mucosa of the mice, the PI3K/Akt pathway will be activated after *Pten* deletion, and *Tgfbr1* loss enhances the paracrine effect of TGF-β in stromal cells [31,32]. After tamoxifen induction, mice with *Tgfbr1* and

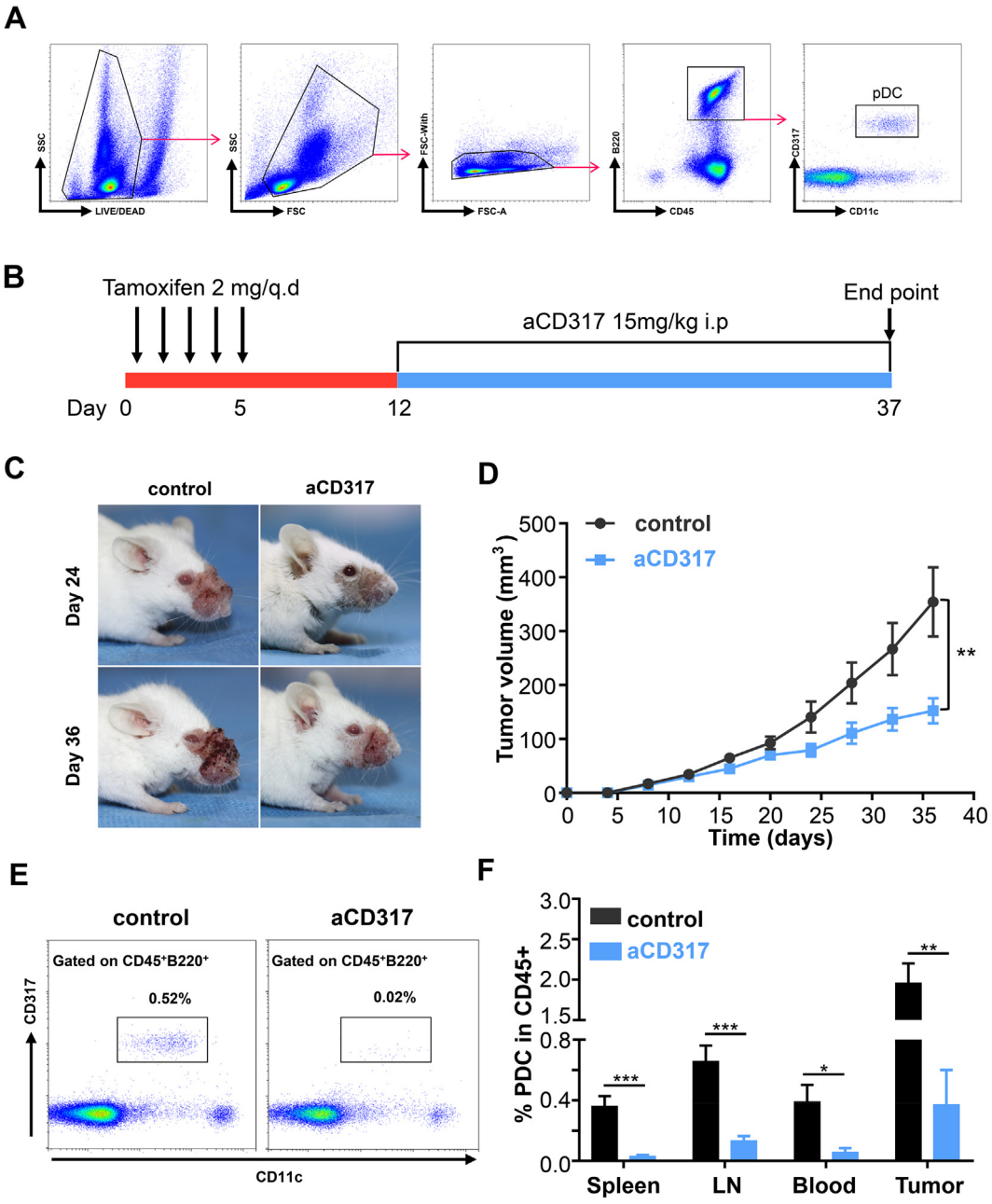

Fig. 1. pDC depletion retarded tumor growth in transgenic HNSCC mouse model. (A) Gating strategy of $CD45^+B220^+CD11c^{low}CD317^+$ pDCs in peripheral immune organs of *Tgfbr1/Pten* 2cKO mouse. (B) Experimental protocol of tumor induction and pDC depletion. (C) Representative photographs of mice with HNSCC in control and pDC depletion group at day 24 and day 36. (D) Growth curves of established tumors in control and pDC depletion groups. 6 mice per group. **, $P < 0.01$. (E) Flow cytometry dot plots showed pDC depletion efficacy in HNSCC mouse model. Cells were gated on $CD45^+B220^+$. (F) Quantification analyses showed pDC depletion efficiency in spleen, draining lymph node, blood and tumor microenvironment. **, $P < 0.05$, **, $P < 0.001$, ***, $P < 0.001$.

Pten combined knockout develop spontaneous tumors with full penetration [23,24]. This mouse model displays pathology and molecular characteristics similar to those seen in human HNSCC [23]. Notably, increased inflammation and immunosuppression can be observed in the tumor microenvironment of this mouse model [23], which makes the mice suitable for this study. pDCs were identified as $CD45^+B220^+CD11c^{low}CD317^+$ cells and detected in this mouse model by multiplex flow cytometry (Fig. 1A). Based on above mentioned that pDC may play a negative role in tumor microenvironment, we speculated that depleting pDCs might exert a positive antitumor effect. To test this hypothesis, pDCs were depleted through applying in vivo CD317 mAbs [25–27]. After tamoxifen-induced tumor initiation, mice were randomly assigned into the pDC depletion group and the control group from day 12 (Fig. 1B). Tumor sizes were monitored, and mice were photographed regularly. Compared with the control group, CD317 mAbs treated group showed a decreased progression rate (Fig. 1C, D). After mice were euthanized, we evaluated the pDC depletion efficacy in the mice. Flow cytometry results showed that the proportion of pDC was markedly decreased (Fig. 1E, F). A decrease in the tumor cell proliferative capacity (as indicated by Ki-67 expression) was detected in the pDC depletion group (Fig. S1A). Considering that pDC may be functionally needed outside the tumor, we primarily assessed the adverse effect of pDC depletion by monitoring body weight changes. The mouse weights in the pDC depletion group were approximately 0.8 g lower than those of the control group mice, though no significant difference was observed (Fig. S1B). We also observed the dysregulation of

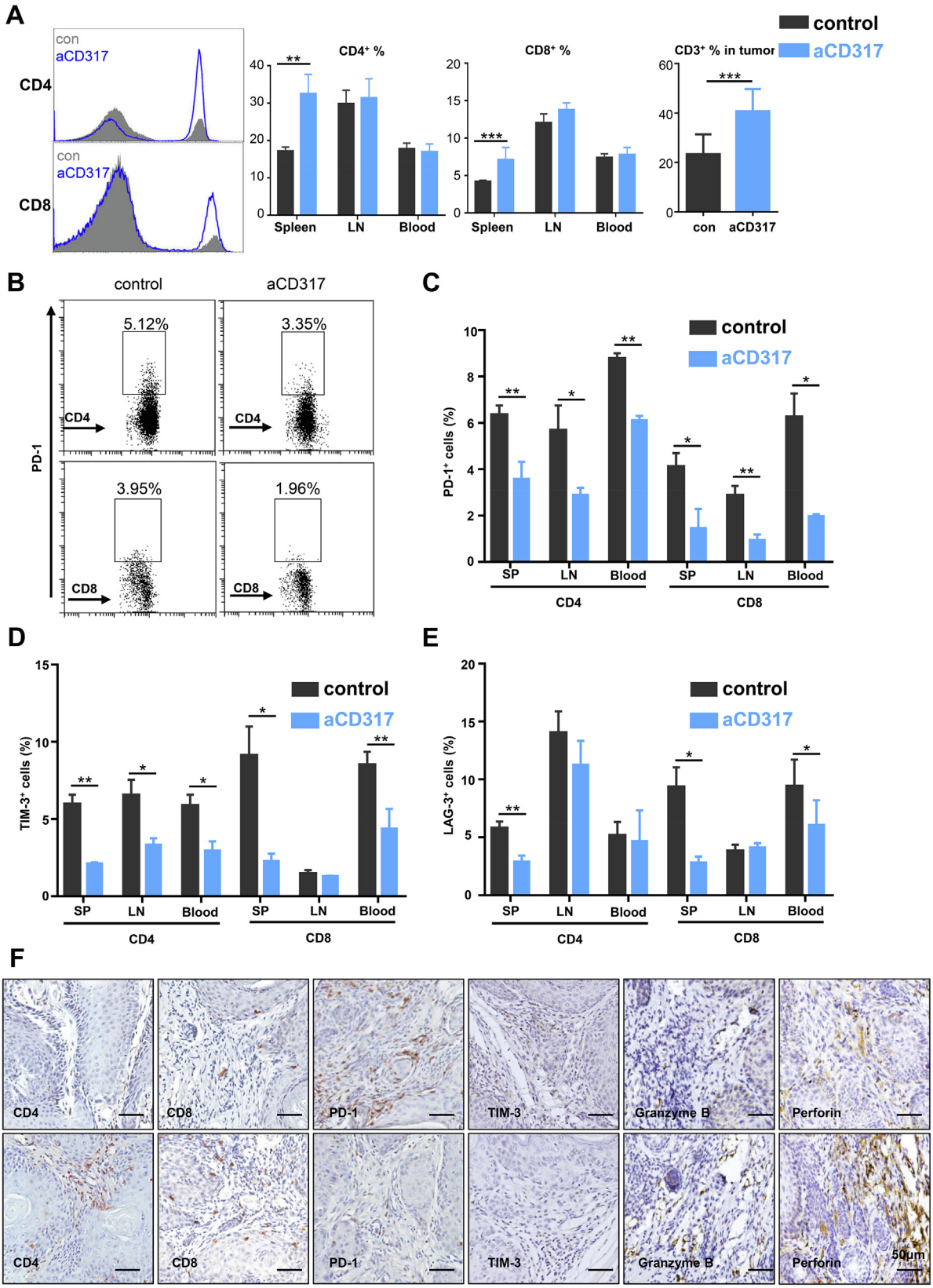

Fig. 2. pDC depletion increased T cell population and reduced immune checkpoints expression in HNSCC murine model. (A) Representative flow cytometric histogram and quantitative analysis of $CD4^+$ and $CD8^+$ T cells in control and pDC depletion groups. Representative flow cytometry plots (B) and quantification analyses (C) showed down-regulated expression of PD-1 on $CD4^+$ and $CD8^+$ T cells after pDC depletion. Quantification analysis of down-regulated expression of TIM-3 (D) and LAG-3 (E) on T cell subsets in the spleen, draining lymph node and blood. (F) In the tumor samples, immunohistochemical staining indicated an increase of CD4, CD8, granzyme B, and perforin staining, and a decrease of PD-1 and TIM-3 staining in aCD317 group compared with control group.

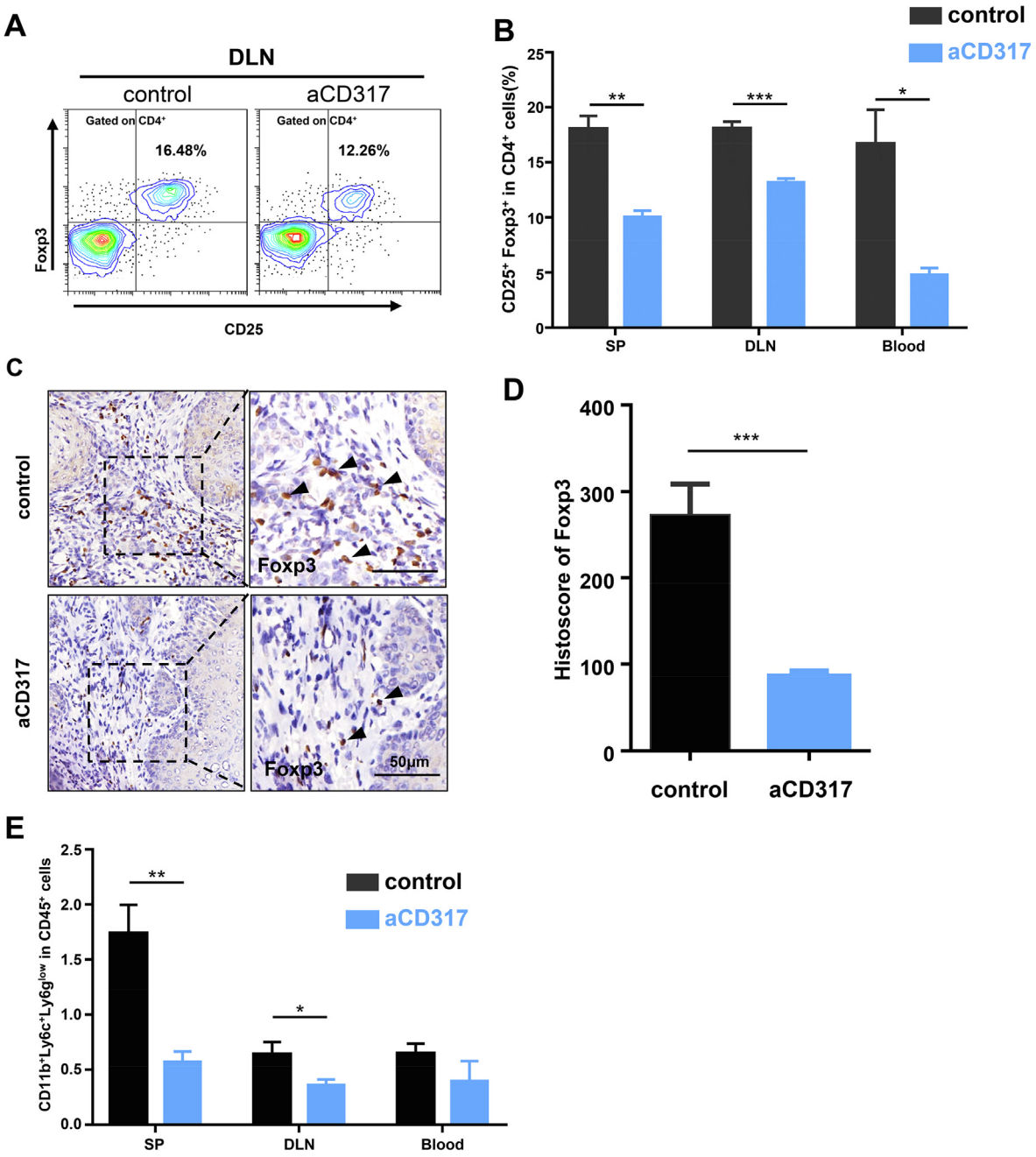

Fig. 3. pDC depletion can decrease the population of Tregs in HNSCC murine model. Representative flow cytometric plots (A) and quantitative analysis (B) of Tregs in control and pDC depletion groups. Immunohistochemical staining (C) and quantitative analysis (D) of Foxp3 in control and pDC depletion groups. (E) Quantification of flow cytometry results showed percentage of $CD11b^+Ly6G^-Ly6C^{high}$ cell in $CD45^+$ cells in the spleen, lymph node and blood of control and pDC depletion groups.

immune organs in the 2cKO tumor-bearing mice, in which the tumor harboring mice exhibited the characteristics of splenomegaly (Fig. S1C) and enlarged lymph nodes (Fig. S1D). After pDC depletion, the size of spleen and lymph nodes was reduced, which to some extent indicated the normalization of immune tolerance status (Fig. S1C, D).

Effect of pDC depletion on T cell revitalization in the transgenic mouse model

In HNSCC, elevated expression of immune checkpoint receptors, including PD-1, TIM-3, and LAG-3, on T cells indicates an immunosuppressive status and contributes to tumor progression [4]. The same effect has been demonstrated in our immunocompetent transgenic HNSCC mouse model [11,12,33]. We investigated the potential impact of pDC depletion on T cell populations using flow cytometric analysis. In the spleen of tumor-bearing mice, pDC depletion could markedly increase the $CD4^+$ and $CD8^+$ T cell populations (Fig. 2A). The upregulation of $CD3^+$ T cells (including $CD4^+$ T and $CD8^+$ cells) was also observed in tumor (Fig. 2A). However, no obvious change was detected in the lymph nodes and blood (Fig. 2A). As pDC depletion can increase the cell populations in the T cell subsets described above, we further investigated whether pDC depletion has an impact on immune checkpoint expression and effecter T cell populations. We determined the expression of three major checkpoint molecules (PD-1, LAG-3 and TIM-3) on T cell subsets in the control and pDC depletion groups in vivo. Notably, the results indicate that the expression of PD-1 (Fig. 2B, C), TIM-3 (Fig. 2D) and LAG-3 (Fig. 2E) on circulating T cells was down-

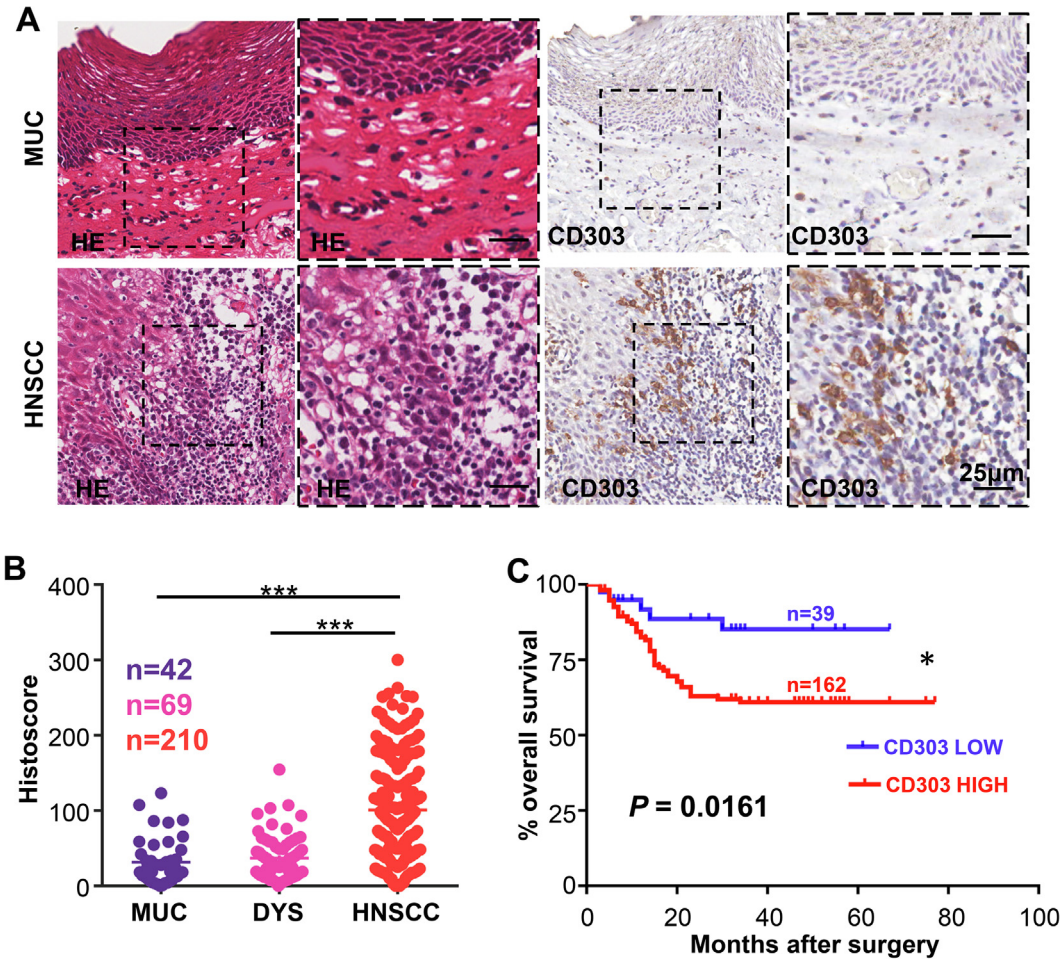

Fig. 4. pDCs (CD303-expressing cells) are highly infiltrative in HNSCC and indicate a poor prognosis. (A) These images showed representative hematoxylin and eosin (HE) and immunohistochemical staining of CD303 in normal mucosa (MUC) and HNSCC samples. Scale bars represent 25 μm. (B) Quantification analyses of the CD303 expression level in HNSCC samples (n = 210), dysplasia samples (DYS, n = 69), and normal mucosa samples (MUC, n = 42). ***, $P < 0.001$. (C) Survival analysis using the Kaplan–Meier method indicates that high expression of CD303 with respect to the optimal cutoff histoscore (histoscore = 39.54) confers a poor prognosis in HNSCC patients. $P = 0.0169$.

regulated after pDC depletion. Immunohistochemical staining of CD4, CD8, PD-1, and TIM-3 further confirmed the T cell population increase and the immune checkpoint downregulation in tumor microenvironments (Fig. 2F). In addition, granzyme B and perforin (markers of T cell effector function) were upregulated in the tumor microenvironment of pDC depletion group. Collectively, these results demonstrate that pDC depletion could revitalize exhausted T cells into an effector state and increase the influx of effector cells into the tumor microenvironment and peripheral immune organs.

pDC depletion reduced the population of Tregs and monocytic MDSCs in the transgenic mouse model

We also investigated immunosuppressive cell types such as Tregs and MDSCs in the control and pDC depletion groups. As shown in Fig. 3A and B, Tregs were remarkably down-regulated in peripheral immune organs including spleen, draining lymph nodes and blood in HNSCC model mice. Immunohistochemical analysis showed consistent results: Foxp3 expression in the tumor microenvironment in mice in the pDC depletion group was significantly reduced (Fig. 3C, D). The population of MDSCs was also determined in this experiment. The results showed that the population of monocytic MDSCs ($CD11b^{+}Ly6G^{-}Ly6C^{high}$) in the peripheral immune organs was decreased (Fig. 3E). In tumor microenvironment, monocytic myeloid-derived suppressor cells (M-MDSCs) rapidly differentiate into tumor associated macrophages and inflammatory DCs [6,34,35]. In our previous study, almost no M-MDSCs were detected in the tumor microenvironment of this mouse model [36]. Thus, M-MDSCs were not detected in the tumor microenvironment.

High levels of pDC infiltration in human HNSCC tumor microenvironments confer a poor prognosis

Based on the effect of pDC depletion in HNSCC mouse model, the infiltration signature of pDC need to be further investigated in human HNSCC. Flow cytometry results showed the existence of pDC in HNSCC (Fig. S2A) and that CD123 positive cells tend to be more mature compared with CD303 positive cells (Fig. S2B, C). Multiple markers have been used to define the maturation stage of pDC including CD80, CD83, CD86, and PD-L1 [18,19,37]. Flow cytometry analysis showed that CD123 positive cells expressed higher levels of CD80, CD83, CD86, and PD-L1 compared with CD303 positive cells (Fig. S2B). In addition, Ki-67 has been used as a marker of immature pDCs [38]. The results of immunostaining in HNSCC tumor microenvironment showed that a large part of CD303 positive cells were Ki-67 positive (Fig. S2C). We then conducted immunohistochemical staining for CD303 (a specific marker of pDCs in humans [15]) in a tissue microarray. pDCs were mainly infiltrated in the stroma of HNSCC tissue and also observed in cancer nests (Fig. 4A). Quantitative analysis showed that pDC infiltration was remarkably higher in primary HNSCC samples (n = 210) when

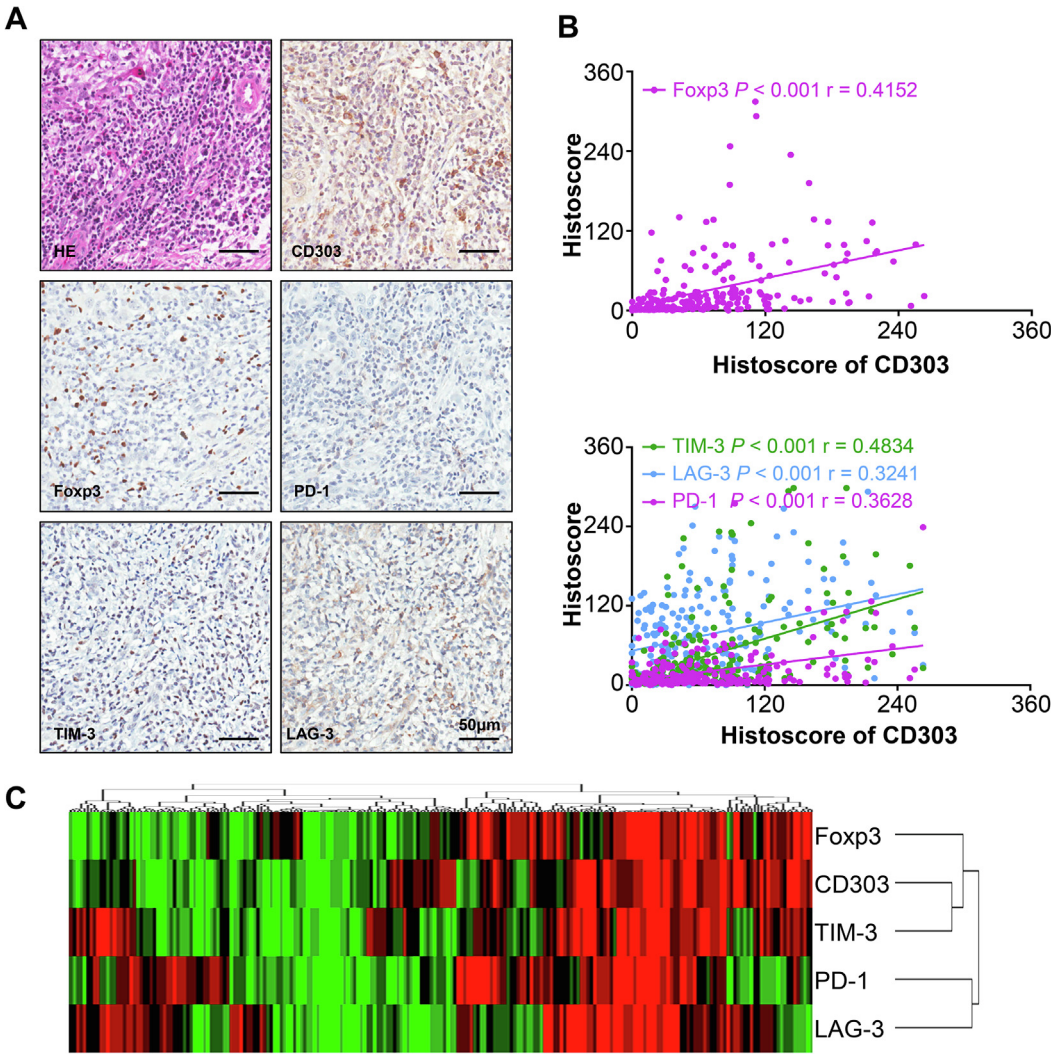

Fig. 5. pDC infiltration is closely related to Foxp3, PD-1, TIM-3 and LAG-3 expression. (A) These images showed representative HE and immunohistochemical staining of CD303, Foxp3, PD-1, TIM-3 and LAG-3 in HNSCC tissue microarray. Scale bars represent 50 μm. (B) Correlation of CD303 expression with Foxp3 ($P < 0.001$, r = 0.4152), PD-1 ($P < 0.001$, r = 0.3628) TIM-3 ($P < 0.001$, r = 0.4834) and LAG-3 ($P < 0.001$, r = 0.3241) expression in a human HNSCC tissue microarray. (C) Hierarchical clustering of the CD303, Foxp3, PD-1, TIM-3, and LAG-3 histoscore results in human HNSCC.

comparing with dysplasia samples (n = 70) and adjacent normal mucosa samples (n = 42) ($P < 0.001$, Fig. 4B). The prognostic implications of pDC infiltration were also evaluated in this HNSCC patient cohort. With respect to the optimal histoscore cutoff (histoscore = 39.54), HNSCC patients with a high level of pDC infiltration had a poorer survival rate than patients with low level of pDC infiltration ($P = 0.0161$, Fig. 4C). Further analyses revealed no significant difference in pDC infiltration among histological grades I, II and III (Fig. S3A), tumor sizes (T1, T2, T3 and T4; Fig. S3B), or lymph node status (N0, N1 and N2; Fig. S3C). In addition, pDC infiltration was decreased in patients who received chemotherapy or radiotherapy ($P = 0.0550$, Fig. S3D; $P = 0.0285$, Fig. S3E).

pDC infiltration was positively correlated with PD-1, TIM-3, LAG-3 and Foxp3 expression in human HNSCC

To further verify the immune-related signature of pDC in HNSCC, we conducted immunohistochemical staining for Foxp3 (a marker of Tregs), immune checkpoints, and other immune-related markers in the HNSCC tissue microarray. Notably, the immunohistochemical staining images (Fig. 5A) and quantification analyses (Fig. 5B) revealed that pDC infiltration was positively correlated with Foxp3 ($P < 0.001$, r = 0.4152), PD-1 ($P < 0.001$, r = 0.3628), LAG-3 ($P < 0.001$, r = 0.3241), and TIM-3 ($P < 0.001$, r = 0.4834) staining. The close association between pDC and TIM-3 expression was further demonstrated through hierarchical clustering (Fig. 5C).

Discussion

Accumulated recent evidence indicated that immune suppressive cells could be manipulated by tumor cells to escape from the immune surveillance [5,7]. pDC has been reported to infiltrate the tumor microenvironment in HNSCC and the capacity to secret IFN-α was suppressed by tumors [22]. In this study, pDC depletion induced by CD317 blockade in the HNSCC mouse model markedly decreased tumor formation and effectively ameliorated the immunosuppressive state in the tumor microenvironment. Further results in human HNSCC revealed that pDC infiltration positively correlated with immune suppressive markers and conferred a poor prognosis.

Tgfbr1 loss in our HNSCC mouse model contributes to the accumulation of TGF-β in stroma [32], which may inhibit the production of type I interferon by pDCs and promote tumor growth [18]. In this study, we observed the presence of pDCs in *Tgfbr1/Pten* 2cKO HNSCC model mice. Thus, we tried to deplete pDCs in this HNSCC mouse model and to

explore whether this treatment would exert an antitumor effect by reversing the immunosuppressive status in the tumor microenvironment and macroenvironment. Our previous study revealed the expression of CD317 on tumor cells [39]. At the same time, CD317 antibodies have been used for depleting pDC in mouse [26,27]. In this work, pDCs were efficiently depleted through applying CD317 antibodies. Interestingly, tumor growth was notably slowed, and the immune organs tended to normalize after CD317 blockade.

Immune checkpoint blockade therapy has shown great promise in treating diverse cancer types including HNSCC [40,41]. In HNSCC patients and in our tumor model, several immune checkpoints, such as PD-1, TIM-3, and LAG-3, have been investigated and found to be overexpressed on tumor-infiltrating cells. Notably, we found that the T cell population was significantly increased in the spleen and tumor microenvironment after pDC depletion induced by CD317 blockade. Furthermore, the expression of PD-1, TIM-3 and LAG-3 was markedly decreased in the tumor macroenvironment and microenvironment, which indicated the revitalization of T cell function.

Initial studies in HNSCC showed that Tregs and MDSCs promote cancer progression by inhibiting T cell activation and that they are associated with a poor outcome [5,42–44]. The immune environment of tumor-bearing *Tgfbr1/Pten* 2cKO mice is also characterized by an accumulation of Treg and MDSC subsets and maintains a suppressive state [11]. pDCs have been demonstrated to directly activate Tregs by expressing indoleamine 2,3-dioxygenase (IDO) in mouse tumor-draining lymph nodes [45]. Tregs were consistently expanded when pDCs were cocultured with tumor-associated $CD4^+$ T cells [46]. Our study indicated that Tregs were markedly decreased in the tumor microenvironment and peripheral immune organs. Moreover, consistent with the findings in a breast cancer mouse model [25], monocytic MDSCs ($CD11b^+Ly6G^-Ly6C^{high}$) were decreased after pDC depletion. Correlation analysis in human HNSCC further confirmed the close correlation of pDC with the markers of Tregs and MDSCs. Spleen could act as a special niche for promoting myeloid hematopoietic stem/progenitor cells differentiation into potent myeloid suppressor cells [47]. In this study, we observed splenomegaly in tumor bearing mice and the size of spleen could be significantly reduced after pDC depletion treatment, which may indicate that pDC depletion could normalize the immune system through downregulating the monocytic MDSC population.

CD123 expression has been used as an indicator of pDC infiltration, and its high expression has been demonstrated to indicate poor survival in primary oral squamous cell carcinoma [48]. While, CD123 can also be expressed by basophils and conventional dendritic cells. We demonstrated that CD123 positive cells were in a more mature stage compared with CD303 positive cells. CD303 is a specific marker of pDC and represents an immature phenotype [15]. In this study, CD303 was used to detect pDCs, and this analysis further demonstrated the high infiltration and adverse implication of pDCs on survival in human HNSCC. The infiltration of pDCs was decreased in HNSCC patients with radiotherapy and chemotherapy. To avoid the interference of chemotherapy and radiotherapy on the prognostic role of pDC, only primary HNSCC patients were included in the survival analysis.

Taken together, our study showed that pDC depletion induced by CD317 blocked restrained tumor progression in the HNSCC mouse model. The immunosuppressive status was also ameliorated in the tumor microenvironment and macroenvironment in HNSCC mouse model after pDC depletion. In addition, pDC high infiltration correlated with an adverse outcome in human primary HNSCC patients. These data suggest that immunotherapy targeting pDCs might be effective in future application for HNSCC treatment.

Acknowledgements

This project was founded by the National Natural Science Foundation of China 81874131, 81672668, 81672667, and Hubei Province Natural Science Funds for Distinguished Young Scholar 2017CFA062.

Conflict of interest statement

None declared.

Appendix A. Supplementary material

Supplementary data to this article can be found online at https://doi.org/10.1016/j.oraloncology.2019.07.019.

References

[1] Siegel R, Naishadham D, Jemal A. Cancer statistics, 2012. CA Cancer J Clin 2012;62:10–29.
[2] Nor JE, Gutkind JS. Head and neck cancer in the new era of precision medicine. J Dent Res 2018;97:601–2.
[3] Quail DF, Joyce JA. Microenvironmental regulation of tumor progression and metastasis. Nat Med 2013;19:1423–37.
[4] Ferris RL. Immunology and immunotherapy of head and neck cancer. J Clin Oncol 2015;33:3293–304.
[5] Strauss L, Bergmann C, Gooding W, Johnson JT, Whiteside TL. The frequency and suppressor function of CD4 + CD25highFoxp3 + T cells in the circulation of patients with squamous cell carcinoma of the head and neck. Clin Cancer Res 2007;13:6301–11.
[6] Veglia F, Perego M, Gabrilovich D. Myeloid-derived suppressor cells coming of age. Nat Immunol 2018;19:108–19.
[7] Gabrilovich DI, Nagaraj S. Myeloid-derived suppressor cells as regulators of the immune system. Nat Rev Immunol 2009;9:162–74.
[8] Whiteside TL. Head and neck carcinoma immunotherapy: facts and hopes. Clin Cancer Res 2018;24:6–13.
[9] Kondo Y, Ohno T, Nishii N, Harada K, Yagita H, Azuma M. Differential contribution of three immune checkpoint (VISTA, CTLA-4, PD-1) pathways to antitumor responses against squamous cell carcinoma. Oral Oncol 2016;57:54–60.
[10] Pardoll DM. The blockade of immune checkpoints in cancer immunotherapy. Nat Rev Cancer 2012;12:252–64.
[11] Deng WW, Mao L, Yu GT, Bu LL, Ma SR, Liu B, et al. LAG-3 confers poor prognosis and its blockade reshapes antitumor response in head and neck squamous cell carcinoma. Oncoimmunology 2016;5:e1239005.
[12] Liu JF, Ma SR, Mao L, Bu LL, Yu GT, Li YC, et al. T-cell immunoglobulin mucin 3 blockade drives an antitumor immune response in head and neck cancer. Mol Oncol 2017;11:235–47.
[13] Zandberg DP, Strome SE. The role of the PD-L1:PD-1 pathway in squamous cell carcinoma of the head and neck. Oral Oncol 2014;50:627–32.
[14] Chen L, Flies DB. Molecular mechanisms of T cell co-stimulation and co-inhibition. Nat Rev Immunol 2013;13:227–42.
[15] Dzionek A, Sohma Y, Nagafune J, Cella M, Colonna M, Facchetti F, et al. BDCA-2, a novel plasmacytoid dendritic cell-specific type II C-type lectin, mediates antigen capture and is a potent inhibitor of interferon alpha/beta induction. J Exp Med 2001;194:1823–34.
[16] Swiecki M, Colonna M. The multifaceted biology of plasmacytoid dendritic cells. Nat Rev Immunol 2015;15:471–85.
[17] Liu Y. IPC: professional type 1 interferon-producing cells and plasmacytoid dendritic cell precursors. Annu Rev Immunol 2005;23:275–306.
[18] Terra M, Oberkampf M, Fayolle C, Rosenbaum P, Guillerey C, Dadaglio G, et al. Tumor-derived TGFbeta alters the ability of plasmacytoid dendritic cells to respond to innate immune signaling. Cancer Res 2018;78:3014–26.
[19] Sisirak V, Faget J, Gobert M, Goutagny N, Vey N, Treilleux I, et al. Impaired IFN-alpha production by plasmacytoid dendritic cells favors regulatory T-cell expansion that may contribute to breast cancer progression. Cancer Res 2012;72:5188–97.
[20] Jensen TO, Schmidt H, Moller HJ, Donskov F, Hoyer M, Sjoegren P, et al. Intratumoral neutrophils and plasmacytoid dendritic cells indicate poor prognosis and are associated with pSTAT3 expression in AJCC stage I/II melanoma. Cancer 2012;118:2476–85.
[21] Labidi-Galy SI, Treilleux I, Goddard-Leon S, Combes JD, Blay JY, Ray-Coquard I, et al. Plasmacytoid dendritic cells infiltrating ovarian cancer are associated with poor prognosis. Oncoimmunology 2012;1:380–2.
[22] Hartmann E, Wollenberg B, Rothenfusser S, Wagner M, Wellisch D, Mack B, et al. Identification and functional analysis of tumor-infiltrating plasmacytoid dendritic cells in head and neck cancer. Cancer Res 2003;63:6478–87.
[23] Bian Y, Hall B, Sun ZJ, Molinolo A, Chen W, Gutkind JS, et al. Loss of TGF-beta signaling and PTEN promotes head and neck squamous cell carcinoma through cellular senescence evasion and cancer-related inflammation. Oncogene 2012;31:3322–32.
[24] Sun ZJ, Zhang L, Hall B, Bian Y, Gutkind JS, Kulkarni AB. Chemopreventive and chemotherapeutic actions of mTOR inhibitor in genetically defined head and neck squamous cell carcinoma mouse model. Clin Cancer Res 2012;18:5304–13.
[25] Sawant A, Hensel JA, Chanda D, Harris BA, Siegal GP, Maheshwari A, et al. Depletion of plasmacytoid dendritic cells inhibits tumor growth and prevents bone metastasis of breast cancer cells. J Immunol 2012;189:4258–65.
[26] Rajagopal D, Paturel C, Morel Y, Uematsu S, Akira S, Diebold SS. Plasmacytoid dendritic cell-derived type I interferon is crucial for the adjuvant activity of Toll-like

receptor 7 agonists. Blood 2010;115:1949–57.
[27] Le Mercier I, Poujol D, Sanlaville A, Sisirak V, Gobert M, Durand I, et al. Tumor promotion by intratumoral plasmacytoid dendritic cells is reversed by TLR7 ligand treatment. Cancer Res 2013;73:4629–40.
[28] Wu L, Deng WW, Huang CF, Bu LL, Yu GT, Mao L, et al. Expression of VISTA correlated with immunosuppression and synergized with CD8 to predict survival in human oral squamous cell carcinoma. Cancer Immunol Immunother 2017;66:627–36.
[29] Kirkegaard T, Edwards J, Tovey S, McGlynn LM, Krishna SN, Mukherjee R, et al. Observer variation in immunohistochemical analysis of protein expression, time for a change? Histopathology 2006;48:787–94.
[30] Leemans CR, Braakhuis BJ, Brakenhoff RH. The molecular biology of head and neck cancer. Nat Rev Cancer 2011;11:9–22.
[31] Honjo Y, Bian Y, Kawakami K, Molinolo A, Longenecker G, Boppana R, et al. TGF-beta receptor I conditional knockout mice develop spontaneous squamous cell carcinoma. Cell Cycle 2007;6:1360–6.
[32] Bian Y, Terse A, Du J, Hall B, Molinolo A, Zhang P, et al. Progressive tumor formation in mice with conditional deletion of TGF-beta signaling in head and neck epithelia is associated with activation of the PI3K/Akt pathway. Cancer Res 2009;69:5918–26.
[33] Yu GT, Bu LL, Huang CF, Zhang WF, Chen WJ, Gutkind JS, et al. PD-1 blockade attenuates immunosuppressive myeloid cells due to inhibition of CD47/SIRPalpha axis in HPV negative head and neck squamous cell carcinoma. Oncotarget 2015;6:42067–80.
[34] Ribechini E, Hutchinson JA, Hergovits S, Heuer M, Lucas J, Schleicher U, et al. Novel GM-CSF signals via IFN-gammaR/IRF-1 and AKT/mTOR license monocytes for suppressor function. Blood Adv 2017;1:947–60.
[35] Condamine T, Kumar V, Ramachandran IR, Youn JI, Celis E, Finnberg N, et al. ER stress regulates myeloid-derived suppressor cell fate through TRAIL-R-mediated apoptosis. J Clin Invest 2014;124:2626–39.
[36] Mao L, Zhao ZL, Yu GT, Wu L, Deng WW, Li YC, et al. gamma-Secretase inhibitor reduces immunosuppressive cells and enhances tumour immunity in head and neck squamous cell carcinoma. Int J Cancer 2018;142:999–1009.
[37] Alculumbre SG, Saint-Andre V, Di Domizio J, Vargas P, Sirven P, Bost P, et al. Diversification of human plasmacytoid predendritic cells in response to a single stimulus. Nat Immunol 2018;19:63–75.
[38] Boichuk SV, Khaiboullina SF, Ramazanov BR, Khasanova GR, Ivanovskaya KA, Nizamutdinov EZ, et al. Gut-associated plasmacytoid dendritic cells display an immature phenotype and upregulated granzyme B in subjects with HIV/AIDS. Front Immunol 2015;6:485.
[39] Yang LL, Wu L, Yu GT, Zhang WF, Liu B, Sun ZJ. CD317 signature in head and neck cancer indicates poor prognosis. J Dent Res 2018;97:787–94.
[40] Ribas A, Wolchok JD. Cancer immunotherapy using checkpoint blockade. Science 2018;359:1350–5.
[41] Ferris RL, Blumenschein Jr. G, Fayette J, Guigay J, Colevas AD, Licitra L, et al. Nivolumab vs investigator's choice in recurrent or metastatic squamous cell carcinoma of the head and neck: 2-year long-term survival update of CheckMate 141 with analyses by tumor PD-L1 expression. Oral Oncol 2018;81:45–51.
[42] Chikamatsu K, Sakakura K, Whiteside TL, Furuya N. Relationships between regulatory T cells and CD8+ effector populations in patients with squamous cell carcinoma of the head and neck. Head Neck 2007;29:120–7.
[43] Figueiro F, Muller L, Funk S, Jackson EK, Battastini AM, Whiteside TL. Phenotypic and functional characteristics of CD39(high) human regulatory B cells (Breg). Oncoimmunology 2016;5:e1082703.
[44] Pak AS, Wright MA, Matthews JP, Collins SL, Petruzzelli GJ, Young MR. Mechanisms of immune suppression in patients with head and neck cancer: presence of CD34(+) cells which suppress immune functions within cancers that secrete granulocyte-macrophage colony-stimulating factor. Clin Cancer Res 1995;1:95–103.
[45] Sharma MD, Baban B, Chandler P, Hou DY, Singh N, Yagita H, et al. Plasmacytoid dendritic cells from mouse tumor-draining lymph nodes directly activate mature Tregs via indoleamine 2,3-dioxygenase. J Clin Invest 2007;117:2570–82.
[46] Faget J, Sisirak V, Blay JY, Caux C, Bendriss-Vermare N, Menetrier-Caux C. ICOS is associated with poor prognosis in breast cancer as it promotes the amplification of immunosuppressive CD4(+) T cells by plasmacytoid dendritic cells. Oncoimmunology 2013;2:e23185.
[47] Wu C, Ning H, Liu M, Lin J, Luo S, Zhu W, et al. Spleen mediates a distinct hematopoietic progenitor response supporting tumor-promoting myelopoiesis. J Clin Invest 2018;128:3425–38.
[48] O'Donnell RK, Mick R, Feldman M, Hino S, Wang Y, Brose MS, et al. Distribution of dendritic cell subtypes in primary oral squamous cell carcinoma is inconsistent with a functional response. Cancer Lett 2007;255:145–52.